**Study of the internal structure, instabilities, and magnetic fields in the dense Z-pinch**

Award No. **DE-SC0008824**

**High Energy Density Laboratory Plasmas**
Research area: **Magnetized High-Energy-Density Plasma Physics**
US Department of Energy

**Program manager:** Sean M. Finnegan

# Final Report

Grant period: August 1, 2012 - July 31, 2015
No cost extension to July 31, 2016

Reporting period: August 1, 2012 - July 31, 2016

**Principal Investigator**: V. V. Ivanov
Research Associated Professor
University of Nevada, Reno
Email: ivanov@unr.edu; Phone: (775)-682-9745

**Recipient Organization:** Board of Regents, NSHE, obo University of Nevada, Reno
**Address**: 1664 North Virginia Street, Sponsored Projects/ MS 325, Reno, NV 89577
**The technical and business point of contact:** Office of Sponsored Projects,
University of Nevada, Reno; **Phone:** (775)-784-4040**; e-mail:** ospadmin@unr.edu

Submitted in August 17, 2016

**Table of contents**



## 1. ACCOMPLISMENTS

The major goal of the project is the investigation of the internal structure, plasma dynamics, and magnetic fields in the stagnated Z-pinch. This goal is based on the development of new UV diagnostics for dense plasmas including diagnostic for MG magnetic fields.

For the first year of the project we planned to develop UV plasma diagnostics and study the stagnated Z pinches as it written in the proposal:

*"Two-frame high-resolution UV shadowgraphy will be designed, tested in the laboratory, and installed at the Zebra generator. Development of 3D structure of the Z pinch at stagnation will be studied in different wire arrays. Fast dynamics of the stagnated dense Z pinch will be studied with 2-frame UV shadowgraphy and interferometry. Mid-scale and small-scale instability will be investigated. Plasma dynamics and instability in the pinch will be modeled with the 3D MHD Gorgon code. Physical mechanisms for small-scale plasma instability will be studied. Faraday rotation diagnostics will be tested in the laboratory. The optimized optical scheme will be installed at the Zebra generator. The first experiments will be carried out with the UV Faraday rotation diagnostics. A sub-nanosecond master oscillation will be installed for the Tomcat Nd:glass diagnostic laser and synchronized with the Zebra generator."*

For the second 2-year period of the grant we planned " *... to study the internal structure of MG magnetic fields in the stagnated Z pinch and investigate hot spots with extreme plasma parameters in different types of wire arrays and X pinches. The extended set of UV and x-ray diagnostics will be used in experiments and new deep UV diagnostics at the wavelength of 211 nm will be designed. We will study fast plasma motion at stagnation which produces enhanced plasma radiation in the Z pinch. The origin, evolution, and collapse of hot spots in the Z pinch will be investigated. Magnetic fields in Z pinches will be analyzed and compared with MHD simulations. Dynamics of plasma instabilities, necks, and hot spots will be simulated with the 3D MHD Gorgon code in Imperial College.*

*The proposed researches are based on new plasma diagnostics. A Tomcat laser will be completed for operation at 266 nm with energy >1.5J and pulse duration of 150ps. The laser will be synchronized for experiments with the Zebra generator and other plasma diagnostics. The Tomcat laser will be implemented for magnetic fields measurements at 266nm and for the multiframe UV diagnostics. Generation of the 5$^{th}$ harmonic in the Tomcat laser will be optimized and the beampath to the Zebra generator will be designed.*

*Capability of diagnostics at the wavelength of 211nm for dense plasma will be demonstrated. Fast laser-driven Kerr shutter for diagnostics of plasma will be investigated.*

*The magnetic field in necks on the stagnated Z-pinch will be studied with UV Faraday rotation diagnostics. Dynamics of hot spots will be investigated with x-ray imaging and streak camera in soft and keV x-ray ranges. Hot spots will be studied in different wire-array configurations to find the highest magnetic fields in the 1 MA Z pinch. Magnetic field will also be studied at current of 1.5 MA with a current doubler. The plasma electron density and temperature in hot spots will be estimated with x-ray spectroscopy. We will carry experiments for laser initiation of the hot spot in the wire-array Z pinch.*

*Four-frame UV diagnostics will be developed. Multiframe diagnostics can deliver data for future development of the UV laser tomography of dense plasmas. End-on Faraday and Cotton-Mouton diagnostics will be applied for investigation of the axial component of the magnetic field in Z pinches.*

*The development of instabilities, magnetic fields, and current distribution will be modeled with the 3D MHD Gorgon code. The code will be upgraded and benchmarked for detailed simulations of the stagnated Z pinch. The enhanced heating of Z-pinch plasma will be analyzed using experimental data and identified with specific physical mechanisms. Hot spots will be modeled and plasma parameters in hot spots calculated."*

Experiments were carried out at the Nevada Terawatt Facility (NTF) during 2-3-week experimental campaigns. Three campaigns at the 1 MA Zebra generator were carried out at the first year of the grant period. One campaign with the Zebra generator and two campaigns with the Zebra generator and Tomcat laser were carried out in the second year. Four experimental campaigns were carried at NTF during the third year including one campaign with the Leopard laser. Two campaigns with the Zebra generator and the Leopard laser were completed in the fours year.

## 1.1. Development of laser diagnostics for dense plasma

### 1.1.1. UV and deep UV laser diagnostics

Laser diagnostics at NTF were redesigned to study plasma dynamics in stagnated *Z*-pinches with high spatial resolution. UV diagnostics provided two-frame shadowgraphy and interferometry. Spatial resolution of diagnostics was 12 μm with the medium magnification and 4 μm at high magnification. A delay between two frames varied from 2.7 ns to 10 ns. A crystal wedge splits the laser beam after the vacuum chamber to ordinary and extraordinary waves with orthogonal polarizations and different angles of propagation. Ordinary and extraordinary waves carried two pulses with orthogonal polarizations. The optical axis of the crystal wedge was parallel to polarization of one frame in this configuration. The crystal wedge provided a high contrast of frames with orthogonal polarizations. Details and schematics of two-frame high-resolution diagnostics at 266 nm were published in Refs. [8,12] in Chapter 2 of this report.

Four synchronized UV channels were used to study asymmetry of the Z pinch produced by different wire arrays [2]. UV diagnostics were used to control the implosion quality and study radiative cooling in the mixed Z-pinch plasma [7].

A UV Faraday rotation diagnostic at 266 nm was applied, at the first time, for measuring of MG magnetic fields in the Z pinch. A three-channel polarimeter included the Faraday and shadowgraphy channels for measurement of the rotation angle and a differential interferometer. Faraday diagnostics were used for qualitative [6] and quantitative [5,9] study of magnetic fields in plasma. A crystal wedge was used to split orthogonal polarizations in Faraday rotation diagnostics. All channels of laser diagnostics were co-aligned using the removable needle in the center of the wire array. The magnetic field was studied in Z pinches and X pinches at current up to 1.5 MA.

A further development of laser diagnostics for dense plasmas was provided by implementing of deep UV diagnostics at the fifth harmonic of the neodymium laser [3]. Dense plasma is more transparent at the UV wavelength due to the increment of inverse bremsstrahlung absorption in plasma and refraction angle on density gradients are proportional to $\lambda^2$. At the first time, we

applied laser diagnostics at the wavelength of 213 nm to Z-pinch and laser produced plasmas. Laser harmonics were generated during the three-step conversion in non-linear crystals. Generation of the 5th harmonic was performed by the frequency mixing of fundamental and fourth harmonics in the BBO crystal. Pulses at four wavelengths propagated together in one beampath, so, deep UV diagnostics was used as a part of four-color diagnostics with frames at wavelengths of 1064, 532, 266, and 213 nm [3]. Pulses were delivered to the vacuum chamber of the Zebra generator located at the distance of 25 m. The absorption of light at the 5th harmonic in air (mostly, by ozone and water vapors) was found at the acceptable level. After the vacuum chamber, laser pulses were split to appropriate CCD cameras by harmonic separators. Multicolor laser diagnostics show plasma in a wide range of densities in one laser shot. Shadowgraphy, interferometry, and schlieren diagnostics were tested in different channels.

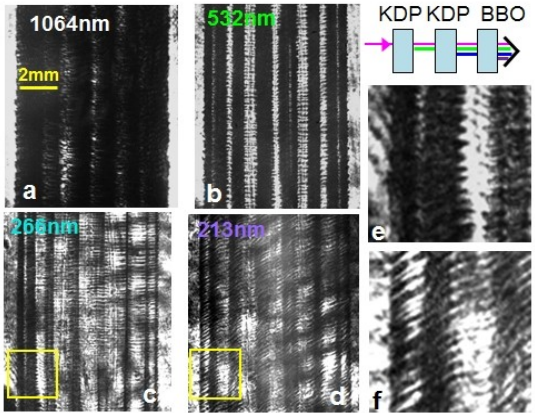


Fig. 1. A 4-color shadowgram of the Al 16-wire cylindrical array at the ablating stage (a) at 1064 nm, (b) at 532 nm, (c) at 266 nm, and (d) at 213 nm. Images (e) and (f) are magnified rectangles in images (c) and (d). A pictogram shows frequency conversion.

Figure 1 from Ref. [3] shows a 4-color shadowgram of the 16-wire cylindrical array at the ablation stage. Images display different plasma features. A shadowgram (a) at the fundamental frequency shows low density plasma in the wire-array volume. Shadowgram (b) taken at the 2nd harmonic identifies wide ablating plasma columns and horizontal jets streaming toward the center. A shadowgram (c) at the 4th harmonic shows narrow dense cores of plasma columns, a precursor, and ablating jets. A shadowgram (d) taken at the 5th harmonic gives more details of dense plasma cores. This shadowgram presents the first application of the deep UV laser diagnostic to Z-pinch plasma. Comparison of magnified fragments (e) and (f) shows that image at the wavelength of 213 nm can clarify a structure of the dense wire core. In previous experiments, a wire core was available for investigation only by x-ray radiography. Coupled UV and x-ray imaging diagnostics covered a wide range of density in our Z pinch experiments [4].

### 1.1.2. Non-linear optical gating for laser diagnostics

A potential of non-linear optical gating for laser diagnostics of plasma was studied. First, we used a Leopard laser with the pulse duration extended to 20 ps. A fused silica glass plate was used as a non-linear Kerr element. Due to the small non-linear index of refraction of glass, laser intensity >$10^{11}$ W/cm$^2$ was used for gating. A gating glass plate was installed between two crossed polarizers. A probing signal at the second harmonic was used. Two issues were found at this setup. First, a non-linear element must be in vacuum to avoid a laser breakdown of air. Second, a rate of shots was limited by the cooling time of 30 min for 94-mm disc amplifiers and 10 min for 45-mm rod amplifiers of the Leopard laser. This made the alignment procedure long and difficult. In the next series of shots we used a diagnostic laser with a pulse duration of 150 ps and $CS_2$ non-linear liquid, as seen in Fig.2. $CS_2$ liquid has a significantly smaller non-linear constant compared to glass. The re-orientation relaxation time of $CS_2$ is 2 ps. With pump laser energy of 60 mJ on the $CS_2$ cell, a contrast of optical gating was >800. Spatial resolution of the beampath with non-linear

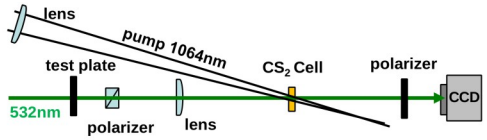


Fig. 2. A setup for laser shadowgraphy with a Kerr optical shutter.

gating was 28 μm. We conclude that fast laser-driving optical shutter with a wide spectral range is attractive for laser diagnostics of plasma. Some non-linear liquids can be used in the UV range.

### 1.1.3. Development of the TOMCAT laser for diagnostics of Z-pinch plasmas

A low-cost project for the development of the Tomcat laser was based on parts of the Nd:glass sub-picosecond laser available at NTF. This narrowband laser was re-designed and re-built for plasma diagnostics and was also applied for investigation of parametric conversion and dynamics of laser produced plasma in the strong magnetic field.

The Tomcat laser is a complementary laser to the Leopard laser at NTF. The Leopard laser operates with a pulse duration of 0.4 ps or 0.8 ns and typical energy of 12 J and 25 J, respectively. A spectral bandwidth of radiation is $\Delta\lambda$=6 nm. Timing of the Leopard laser to the Zebra generator is ±15 ns due the jitter of the Zebra current pulse. Tomcat is a narrowband laser ($\Delta\lambda$ <10 pm) with pulse durations of 150 ps and 2.5 ns and output energy of 3.5 J and 8 J, respectively. The laser pulse is timed to the Zebra current pulse with a jitter of ±2 ns provided by the fast feedback from the Zebra generator sensor. The Tomcat laser consists of the custom Nd:YLF master oscillator and three phosphate glass amplifiers with apertures of 16 mm, 25 mm, and 45 mm. The intensity of the laser pulse at the fundamental harmonic was limited by 2.3 GW/cm$^2$ (3.5 J) in the 150 ps regime due the condition of the output laser rod. This rod was used in previous experiments at NTF in 2007-2010 and has small-scale-focusing bulk damages. KDP crystals were used for conversion to the 2$^{nd}$ and 4$^{th}$ harmonics. Efficiency of 43% was measured for conversion from the 1$^{st}$ to the 2$^{nd}$ harmonic and 35% from the 2$^{nd}$ to the 4$^{th}$ harmonic. The diameter of the BBO crystal for conversion to the 5$^{th}$ harmonic was 2 cm due to limitations of the crystal growing technology. This limited the energy of the 5$^{th}$ harmonic to 25 mJ. Energy of the Tomcat laser at the 4$^{th}$ and 5$^{th}$ harmonics is higher compared to commercial lasers and allows the multichannel laser probing of Z pinches at the Zebra generator.

## 1.2. Investigation of Z pinches at stagnation

### 1.2.1. Small-scale instabilities and plasma dynamics

Experiments for this grant were carried out at the Zebra pulsed power generator at NTF with a rise time of the current pulse of 80 ns and maximum current up to 1.7 MA. Laser diagnostics of plasma included a four-frame shadowgraphy at 532 nm, two-frame UV shadowgraphy/ interferometry and a Faraday rotation diagnostic. Plasma dynamics in the stagnated Z pinch was studied by the two frame diagnostics. Interferograms were processed using Abel inversion. The electron density of (1-3)x10$^{20}$ cm$^{-3}$ was measured directly in the pinch plasma using interferometry at 266 nm [4,8]. Supporting x-ray diagnostics included a time-gated pinhole camera, x-ray diodes, time-integrating spectrometers with a convex KAP crystal and concave quartz and mica crystals, and an x-ray streak camera.

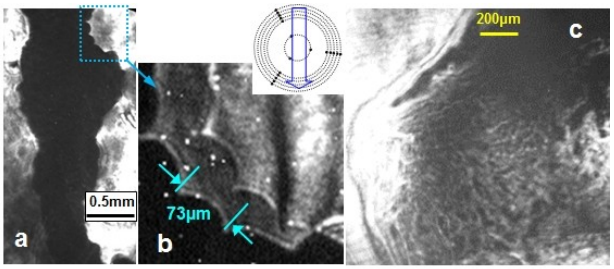


Fig. 3. (a) A wire array Z pinch at stagnation. (b) Mid-scale plasma instability on the pinch. (c) Small-scale plasma instability in the Z pinch [11].

MHD sausage and kink instability are well known in Z pinch physics. Figure 3 shows new small-scale plasma instabilities in the wire-array Z pinch. Images (a) and (b) present a periodical structure on the edge of the pinch. Instability with a period of 70-150 μm may be linked to Magneto-Rayleigh-Taylor instability (MRTI) due to the plasma motion at stagnation. Fig. 3(c) presents "worm"-like density perturbations with a characteristic size of (10-30) x (50-200) μm in

the pinch later after stagnation [11]. These perturbations can be generated during the nonlinear evolution of MHD instabilities or by the flute mode instability.

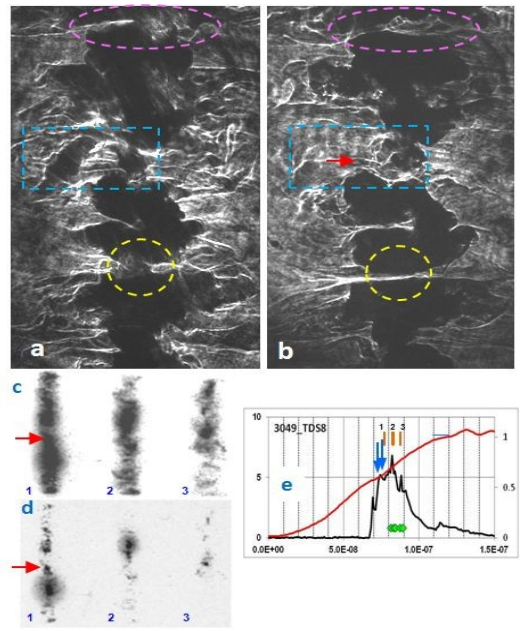


Fig. 4. (a) and (b) Two-frame UV shadowgram. (c) and (d) X-ray frames at E>0.8 keV and E>3 keV. (e) A timing diagram from the implosion of the Al wire array. The timing diagram presents a current pulse (red line), x-ray pulse (black line), UV frames (arrows), and x-ray frames (stripes).

A fast plasma motion in the stagnated Z pinch was observed with two-frame shadowgraphy. Fig. 4 presents the dynamics of necks and bulges on the pinch in the 2-frame shadowgram with 2.8 ns between frames. Three shapes present the same area in two frames. Areas in the yellow circles present development of the break from the neck on the pinch. Areas in the blue rectangles show a disappearance of the plasma arm on the pinch. This may change a configuration of the current flow near the neck. Areas in the pink ovals show evolution of the neck in the pinch gap. Two-frame UV diagnostics show that plasma at stagnation can move with a speed of >100 km/s. The Z pinch in shadowgrams is distorted by the kink and sausage instabilities. X-ray images (c) and (d) present two series of frames with 6 ns between frames. Diagram (e) shows timing of diagnostics. Red arrows on images (b-d) show correlation of the x-ray bright spot with a position of the neck in the UV shadowgram. The electron temperature of plasma calculated from the Al K-shell spectra was in the range of 400-440 eV in hot areas and 270-330 eV in cold areas.

High-resolution UV diagnostics shows the dense Z pinch in unprecedented details. MHD instabilities, areas of disruption, and small-scale density perturbations are well seen in Z pinches during stagnation stage. Plasma dynamics in the dense pinch shows that stagnation is not a static stage but it's a dynamic process with fast moving plasma.

### 1.2.2. A 3D structure and asymmetry of the Z pinch

Experiments with 4-channel side-on UV shadowgraphy and interferometry at 266 nm were conducted at the Zebra generator to study asymmetry of wire-array Z pinches at the stagnation stage. The laser probing directions of four 3-lens identical channels on the vacuum chamber were evenly spaced, in 45° increments and timed with 100 ps accuracy to provide simultaneous imaging of the Z pinch in four directions [2].

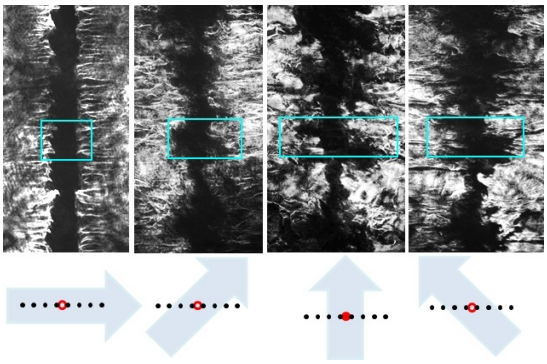

Fig. 5. A 4-channel UV shadowgram of the planar wire array at stagnation.

Azimuthal non-uniformity in cylindrical, star, and linear wire-array Z pinches were studied. Fig. 5 displays a linear wire array imploded to the pinch with high azimuthal inhomogeneity due to the asymmetry of the pinch plasma, instability jets, and trailing material. Images in rectangles show very different pinch plasma in different directions. Shadowgrams confirm that trailing plasma stays in the plane of the line of wires during the

implosion stage in planar arrays. Other types of wire-array Z pinches produced by implosions of cylindrical and star wire arrays present azimuthal asymmetry due to the kink instability and generation of plasma jets.

A spatial profile of Z-pinch plasma can impact interpretation of data from laser and x-ray diagnostics which, typically, collect data from one direction only. Knowing a 3D structure of the pinch helps to understand the physical processes in Z pinches. Multi-channel probing can be a base for the development of deep UV tomography of Z pinches.

### 1.2.3. Faraday rotation measurements of magnetic fields in the Z pinch

The dynamics and distribution of current and magnetic fields in imploding and stagnating plasmas is crucial for Z pinches. A structure of magnetic fields was studied with Faraday rotation diagnostics at the wavelength of 266 nm. The magnetic field and current were reconstructed from Faraday images using Abel inversion. The reconstructed B-field was compared with a model of two current-carrying plasma columns to find a distribution of current [9].

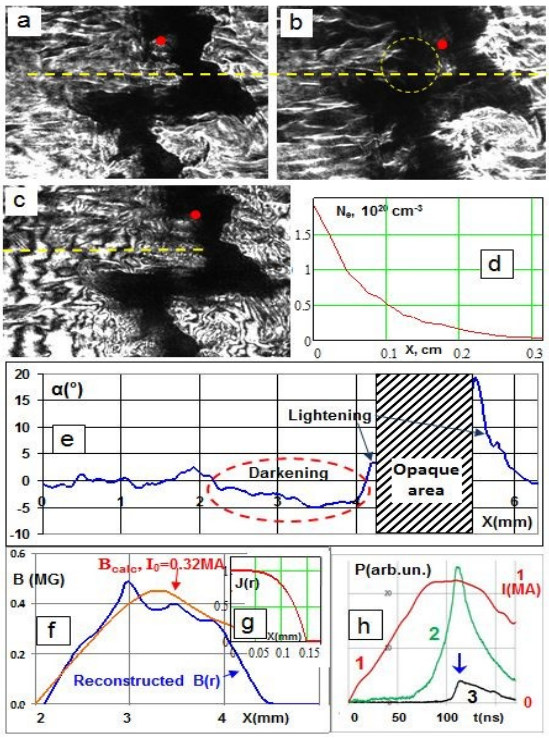


Fig. 6. (a)-(c) A shadowgram, Faraday image, and interferogram of the Al cylindrical wire array Z pinch. (e) The rotation angle calculated along the dashed line in images (a)-(c). (d) The plasma electron density reconstructed from the edge of the opaque zone. (f) The reconstructed magnetic field and the magnetic field calculated with a current density profile (g). (h) The timing diagram for current (1), soft x-ray pulse (2), keV x-ray pulse (3), and UV frames (arrow).

Figure 6 shows images of kink instability in the Z pinch taken by the polarimeter. Faraday image (b) demonstrate lightening in the one side of the pinch and darkening in another side of the image due to the opposite directions of magnetic fields. Darkening in the circle in image (b) indicates an alternative current path in the low-density plasma. Typical angles of rotation of the polarization plane in the pinch are in the range of $\alpha$ = 2-6°. Figure 6 demonstrates (d) the electron density, (e) the rotation angle, and (f) the reconstructed magnetic field in the trailing plasma. Data processing includes several steps. First, a phase shift is calculated from the differential interferogram (c). A radial profile of the electron density is reconstructed with the Abel transform. Second, the rotation angle of the polarization plane is calculated from Faraday image (b), complementary shadowgram (a), and their reference images. Next, the electron density $N_e(r)$ and rotation angle $\alpha(r)$ were used for calculation of $B(r)$ using Abel transform for the magnetic field.

The maximum strength of the magnetic field in the area of darkening is ~0.4 MG. This magnetic field was modeled for current with a parabolic distribution shown in diagram (g). The magnetic field calculated for current $I$ =0.32 MA fits the magnetic field reconstructed in the circle area in Fig. 6 (b). A significant part of 1 MA current flows in trailing material. A redistribution of current can be driven by the increase of the inductance due to the kink instability or micropinching.

The UV Faraday rotation diagnostic was applied to Z pinches at current up to 1.6 MA. Current was increased by the load current multiplier on the pulse-forming-line of the Zebra generator. A radial distribution of the magnetic field and current were reconstructed in the vicinity of the neck

on the pinch [5]. It was found that the main portion of current flows in the large-size trailing plasma with the radius of 2-3 mm. The current density in the narrow dense neck was found to be increased by the factor of 5-10 compared to the trailing plasma that was in agreement with the formation of bright x-ray spots on pinch. We suppose that necks in the wire-array Z pinch are not formed during the compression of the plasma column by the sausage instability. Plasma instabilities at the ablation and implosion stages results in the inhomogeneous implosion and formation of necks at points of collision of plasma bubbles. A distribution of current in the large-size trailing plasma prevents the formation of magnetic fields with $B$ >>1 MG.

The trailing plasma with distributed current can implode and deliver the enhanced kinetic energy in the stagnated pinch. Power of 0.1-0.15 TW can be generated by multiple plasma implosions. This is 10-20% of power radiated by the 3 mm cylindrical wire array due to.

A 3-channel UV end-on polarimeter was applied to Z pinches for investigation of non-azimuthal $B$-fields. The image from the polarimeter accumulates the impact of the Faraday rotation, depolarization on gradients, and Cotton-Mouton ellipticity in plasma. The Cotton-Mouton effect is sensitive to the $B$-field directed orthogonally to the laser wavevector and produces a specific depolarization cross in the image. Cylindrical wire-array Z pinches were studied by the UV end-on polarimeter. The highest depolarization was found in the peripheral plasma associated with collision of imploding plasma with the precursor, so, depolarization can be produced by plasma gradients at shock areas. A depolarization cross was not seen, so, the Cotton-Mouton effect was negligible in our 1 MA Z pinches.

### 1.2.4. Study of micropinches in wire-array Z pinches

Bright and hot spots represent sophisticated HED objects arising in all types of Z pinches. We studied hot spots and micropinches using an x-ray streak camera synchronized with laser and x-ray framing diagnostics [10]. Small-diameter wire arrays were studied because they create pinches with numerous bright spots. UV and x-ray diagnostics showed a difference between the regular necks on the pinch and micropinches (hot spots). Micropinches are presented on the streak image as short peaks with high intensity increased by a factor of 10-30 compared to the background as shown in a 3D plot in Fig. 8 (d). A lifetime of the hot spot in streak images is 0.6-1.5 ns. Typical sizes of hot spots are in the range of 0.3-0.6 mm. Hot spots produce continuum radiation in x-ray spectra which may be linked to bremsstrahlung radiation. Calculations of energy of hot spots from streak images show that a single hot spot can radiate 1-3% of x-ray energy of the wire-array Z pinch with a total contribution from all hot spots of 10-30%.

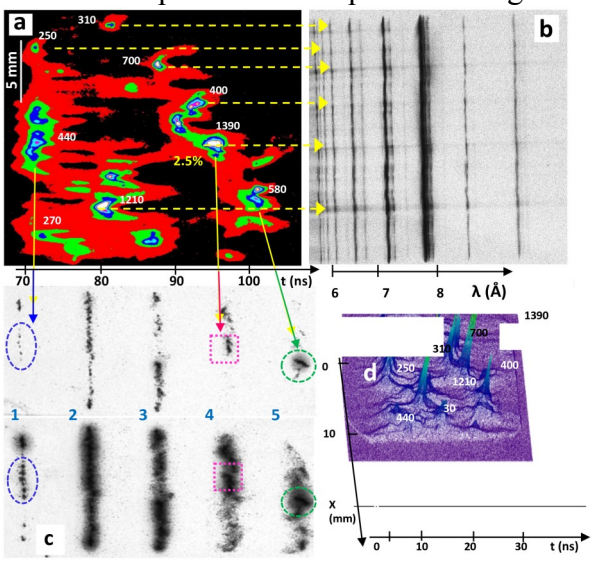


Fig. 8. (a) and (b) A streak image and time-integrated spectrum with axial resolution. (c) X-ray frames of the cylindrical wire array filtered for 3keV (upper row) and 1.2keV (lower row). (d) A 3D plot of the streak image.

Figure 8 (a) shows (a) a false-color streak image, (c) time-gated pinhole images, (b) axially-resolved time-integrated Al K-shell spectra, and (d) a 3D plot of the streak image. Arrows from image (a) to image (b) show correlation of spatial positions of powerful x-ray bursts in the streak image with positions of keV continuums in Al K-shell spectra. This spectral continuum

distinguishes the high-power x-ray sources ("micropinches") from other bright spots on the pinch. Micropinches produce hot spots during the collapse of necks.

The two dashed ovals in Fig. 8(c), frame 1, show "bright spots" from radiation of necks at the beginning of stagnation. Intensity of these bright spots is significantly lower and they do not produce spectral continuum.

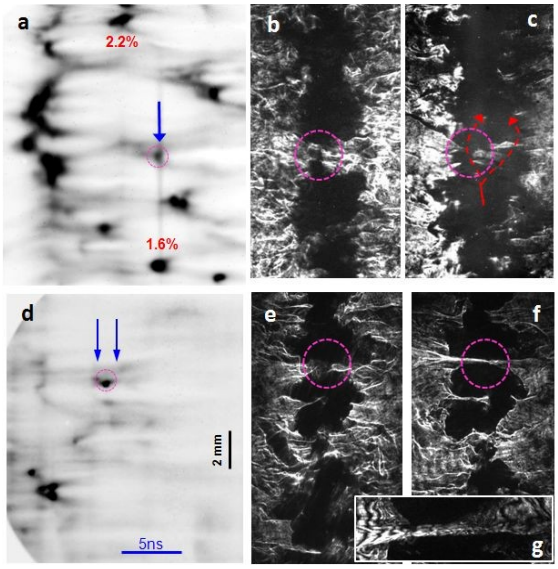


Fig. 9. (a) and (d) Streak images from two shots. (b) and (c) A shadowgram and complementary Faraday image. (e) and (g) A two-frame shadowgram and (g) interferogram.

Figure 9 displays streak images from two shots coupled with UV laser frames [10]. UV diagnostics included three channels of shadowgraphy and interferometry or a Faraday rotation diagnostic. Vertical arrows in streak images (a) and (d) show timing of UV frames. Circles identify spatial positions of micropinches in images. Images (b) and (c) are taken by the Faraday rotation diagnostic at the wavelength of 266 nm. Images (e) and (f) present a 2-frame shadowgraphy. Shadowgram (b) shows a micropinch in the area of the neck. Faraday image (c) shows an area with lightening and darkening in the left to the micropinch which identifies current in the trailing plasma. The split of current may result in lower power radiation of the hot spot in the circle in image (a), compared to other micropinches. A switch of current to the trailing plasma can changes dynamics of the collapse of hot spots.

Fig. 9 (e) and (f) display a two-frame UV shadowgram timed to a streak image. A formation of the micropinch is shown in frame (e) before the micropinch collapse. The second frame (f) is taken 2.8 ns after frame (e) after the collapse of the micropinch. A break in the pinch is produced by the explosion of the hot spot. Fig. 9 clearly shows the origin of the hot spot phenomenon as a collapse of the micropinch on the Z-pinch neck.

### 1.2.5. **3D MHD Gorgon simulations of Z pinch plasma**

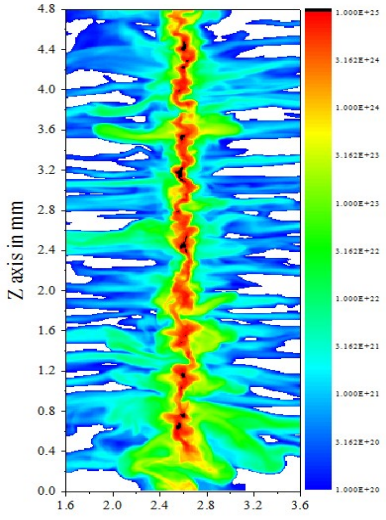


Fig. 10. 3D Gorgon simulation of the $\int n_e dl$ spatial distribution in the stagnated Z pinch.

Simulations with a 3D MHD code Gorgon concentrated on modelling the current distribution during the stagnation phase and instability growth in cylindrical and compact wire arrays. Preliminary work involved the extension of post-processing tools based on non-LTE calculations of emission spectra to allow the generation of synthetic x-ray streak images with various filters, to compare to the experimental observations. Post processing was also used to generate images of $\int n_e dl$ (see Fig.10) and Faraday rotation. These revealed that the typical timescale for the onset of large scale m=1 instability growth was faster in the calculation than in the experiment and gave rise to shorter x-ray pulse durations in simulation. In part this was thought to be the result of the strong radiative cooling rates associated with using an LTE atomic physics and radiation model inline in the MHD code, which enhances the compressibility of the plasma giving rise to tighter pinches and

faster instability growth rates. To address this, the code was adapted to allow the non-LTE model, used for post-processing, to run inline. This required work to improve the accuracy of the non-LTE model in the low temperature regimes required for the cold-start conditions within the cores of the wires used in the array. The introduction of the non-LTE model inline improved agreement with experiment; however it still appeared that the rate of rise of current through the stagnated pinch column was faster in simulation and that this was affecting the instability growth rate. A variety of changes to the initial perturbation on the wires were implemented to increase the amount of trailing mass during the implosion and slow the current delivery to the pinch on axis. It was found that rather than using an entirely random uncorrelated perturbation, allowing a finite degree of correlation of perturbation from wire to wire increased the level of trailing mass and therefore improved agreement. It may be that such an unusual level of correlation is a peculiarity of small diameter arrays with small inter-wire gaps.

3D MHD Gorgon simulations were used to explain plasma instabilities in wire-array Z-pinches at the Zebra generator [8,11], current redistribution, plasma motion, and enhanced heating at stagnation [9], and the formation of micropinches on the Z pinch [10].

### 1.3. A parametric decay of laser radiation in the MG magnetic field

Magnetic fields, $B$=1-2 MG were measured at the Z pinch by Faraday diagnostics. These $B$-fields are too small for application of the Cotton-Mouton and cut-off methods at the Zebra generator. However, another idea for measuring strong magnetic fields was tested. The suggested method is based on two-plasmon conversion of the laser pulse to the 3/2ω scattered radiation. Red- and blue-shifted spectral components of 3/2ω light carries a signatures of both the plasma temperature and magnetic field. In the case of back reflection, a spectral shift in nm can be estimated $\Delta\lambda_{3/2} \sim 2\lambda_0 T_e$, where $\lambda_0$ is a laser wavelength in μm, and $T_e$ is a plasma electron temperature. The magnetic field produce an additional shift $\sim(\omega_{ce})^2/\omega_0$ to the thermal shift of spectral components. The magnetic shift can be observed in the cold plasma if the magnetic field of 3-5 MG.

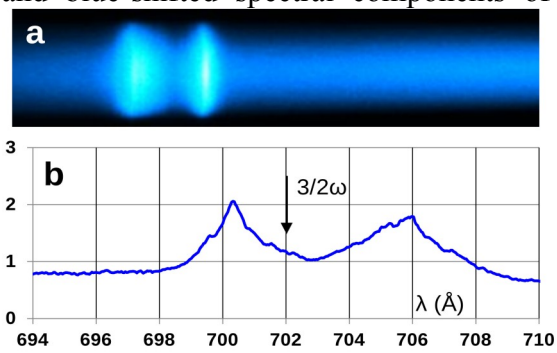


Fig. 11. (a) Time-gated spectrum of the laser plasma on the Al 1mm rod load. (b) A plot of intensity of 3/2ω spectral components.

A proof of principle experiment was carried out at the Zebra generator coupled with a narrowband Tomcat laser. The magnetic field of 2-2.6 MG was generated on the surface of the rod load 1 mm in diameter. A plasma on the surface of this load was cold, $T_e$= 5-15 eV. A 2 ns laser pulse with intensity of $>10^{15}$ W/cm$^2$ was focused on the load surface. Figure 11 shows spectrum of the back-reflected 3/2ω harmonic recorded by the time-gated spectrometer. Spectrum had both blue and red scattered spectral components. A large spectral shift was presumably produced by heating of plasma by the laser. The magnetic and thermal spectral shifts may be separated in future experiments if the spectral dynamics is taken by the streak camera.

The proposed method for measurement of the B-field doesn't require a propagation of radiation through the dense plasma object but uses back scattering from the local area with the electron density of 1/4 of the critical density which is $n_e$=2.5x10$^{20}$ cm$^{-3}$ at 1053 nm and $n_e$=1.1x10$^{22}$ cm$^{-3}$ at 211 nm. The magnetic field of B>10 MG can be measured in plasma by this method.

### 1.4. Laser plasma interaction at the MG magnetic field

Using the experience in generation and measurement of MG fields at the Zebra facility, we studied laser plasma interaction at the external field $B > 2$ MG. Z pinches are not applicable for the controlled experiments due to the high temperature, strong plasma instabilities, and unpredictable configuration of the Z-pinch plasma. A 2-3 MG magnetic field was produced at the Zebra generator by metal rod loads 0.7-2 mm in diameter. Plasma with a steep gradient, electron temperature of 10-15 eV, and high density plasma arises on the surface of the rod load and slowly expands during the current pulse. Radiation of the Leopard laser with intensity of $3 \times 10^{15}$ W/cm$^2$ (0.8 ns/ 18 J at 1056 nm, F/5 lens) was focused on the surface of the load. Side-on shadowgraphy shows the formation of two collimated plasma jets in the magnetic field. The first jet propagates back from the focal spot. The second jet arises on the rear side of the load. In previous studies at smaller $B$=0.1-0.3 MG, a front plasma jet was linked to the ExB drift. The rear jet may be generated by MeV electron beam but our laser intensity is too small. We suppose that laser produced plasma has a shape of a thin disc around the rod load. The formation of the plasma disc in the magnetic field has never been observed before our experiments.

Our experiments showed that laser-plasma interaction in the MG magnetic field is an insufficiently explored field of plasma physics. These type of research require both a MA-class pulsed power machine and a high-intensity laser beam and therefore can only be performed at UNR and Sandia National Laboratories.

## 2. PRODUCTS

### 2.1. Publications and presentations

#### Journal papers


**1.** V. V. Ivanov, A. V. Maximov, R. Betti, P. P. Wiewior, P. Hakel, M. E. Sherrill, "Observation of the disc-like plasma mode during the laser-plasma interaction in a MG external magnetic field", in preparation for publication.

**2.** V. V. Ivanov, A. A. Anderson, "Investigation of asymmetry of wire-array Z pinches at stagnation using a 4-channel laser diagnostic", High Energy Density Physics journal, in press.

**3.** V. V. Ivanov, A. A. Anderson, I. A. Begishev, "Four-color laser diagnostics for Z pinches and laser produced plasma", Applied Optics **55**, 498 (2016).

**4.** A. A. Anderson, V. V. Ivanov, A. L. Astanovitskiy, D. Papp, P. P. Wiewior, and O. Chalyy, "Study of ablation and implosion stages in wire arrays using coupled UV and x-ray probing diagnostics", Physics of Plasmas **22**, 112702 (2015).

**5.** V. V. Ivanov, A. A. Anderson, D. Papp, A. L. Astanovitskiy, V. Nalajala, O. Dmitriev, "Study of magnetic fields and current in the Z pinch at stagnation", Physics of Plasmas **22**, 092710 (2015).

**6.** A. A. Anderson, V. V. Ivanov, D. Papp, "Visualization of the Magnetic Field and Current Path in Z-pinch and X-Pinch Plasmas", High Energy Density Physics **15,** 1-3 (2015).

**7.** V. V. Ivanov, R. C. Mancini, D. Papp, P. Hakel, T. Durmaz, R. Florido-Hernández, "Radiative cooling of two-component wire-array Z-pinch plasma"**,** Physics of Plasmas **21**, 082704 (2014).

**8.** V. V. Ivanov, A. A. Anderson, D. Papp, B. R. Talbot, J. P. Chittenden, N. Niasse, I. A. Begishev, "UV laser probing diagnostics for the dense Z pinch"**,** IEEE Trans. Plasma Sci., **42**, 1153 (2014).

**9.** V. V. Ivanov, A. A. Anderson, D. Papp, A. L. Astanovitskiy, B. R. Talbot, J. P. Chittenden, N. Niasse, "Current redistribution and generation of kinetic energy in the stagnated Z pinch", Phys. Rev. E **88**, 013108 (2013).

**10.** V. V. Ivanov, D. Papp, A. A. Anderson, B. R. Talbot, A. L. Astanovitskiy, V. Nalajala, O. Dmitriev, J. P. Chittenden, N. Niasse, S. A. Pikuz, T. A. Shelkovenko, "Study of micropinches in wire-array Z pinches", Phys. Plasmas **20**, 112703 (2013).

**11.** V. V. Ivanov, J.P. Chittenden, R. C. Mancini, D. Papp, N. Niasse, S. D. Altemara, and A. A. Anderson, "Investigation of plasma instabilities in the stagnated *Z* pinch", Phys. Rev. E **86**, 046403 (2012).

**12.** S.D. Altemara, D. Papp, V.V. Ivanov, A.A. Anderson, A. Astanovitskiy, V. Nalajala, "High-Resolution UV Laser Diagnostics on the 1-MA Zebra Generator", IEEE Trans. Plasma Sci. **40**, 3378 (2012).

### Invited talks

1. V.V. Ivanov, A. A. Anderson, B. S. Bauer, K. Yates, S. Fuelling, T. Hutchinson, J. Mei, "Study of wire-array Z pinches with UV multichannel diagnostics". *The 20th IEEE Pulsed Power Conference*, Austin, Texas, May 31-June 4, 2015.
2. V.V. Ivanov, R. C. Mancini, D. Papp, P. Hakel, R. Florido-Hernández, T. Durmaz, "Radiative properties of two-component plasma produced by implosion of the wire-array Z-Pinch". *The 3rd RHEDP International Workshop*, South Lake Tahoe, NV, June 9-12, 2015.
3. V.V. Ivanov, "UV laser diagnostics for the dense Z-pinch". *The IEEE Pulsed Power Plasma Science Conference,* San Francisco, June 16-21, 2013

### Other presentations of the PI and students from his group

1. V. V. Ivanov, "Laser plasma in a multi-MG magnetic field", Z Fundamental Science Program Workshop, Albuquerque, NM, July 31-August 3, 2016. Oral.
2. V. V. Ivanov, A. V. Maximov, R. Betti, P. P. Wiewior, P. Hakel, M. E. Sherrill, "Formation of the plasma disc during the laser-plasma interaction in a 2-MG magnetic field", 11th International Conference on High Energy Density Laboratory Astrophysics, Menlo Park, Ca, May 16-20, 2016. Poster.
3. V. V. Ivanov, A. V. Maximov, A. M. Covington, P. P. Wiewior, A. L. Astanovitskiy, V. Nalajala, O. Chalyy, O. Dmitriev, "Interaction of laser radiation with plasma in the external MG magnetic field". *57th Annual Meeting of the APS Division of Plasma Physics*, Savannah, GA, November 16-20, 2015. Oral.
4. V. V. Ivanov, A. V. Maximov, A. M. Covington, "Interaction of laser radiation with plasma under the external MG magnetic field". *Frontiers of Plasma Science Workshops*, Town Meeting, Bethesda, MD, June 30–July 1, 2015. Poster.
5. V. V. Ivanov, "Laser diagnostics for Z-pinch plasma", *Seminar at NSTec*, Las Vegas, May 26, 2015.
6. V. V. Ivanov, A. V. Maximov, A. A. Anderson, B. S. Bauer, K. Yates, "Study of strong magnetic fields using parametric instability in a magnetized plasma". *The 56th APS-DPP Meeting*, New Orleans, LA, October 27-31, 2014. Oral.
7. A. Anderson, V. V. Ivanov, "Study of the 3D Structure of the Stagnated Z-Pinch". *The 56th APS-DPP Meeting*, New Orleans, LA, October 27-31, 2014. Poster.
8. V. V. Ivanov, A. A. Anderson, B. S. Bauer, K. Yates, J. P. Chittenden, N. Niasse, A. V. Maximov, **"**Measuring MG magnetic fields in the dense Z pinch". *The Dense Z-pinches Conference*, Napa, August 4-7, 2014. Oral.
9. A. A. Anderson, V. V. Ivanov, A. L. Astanovitskiy, P. Wiewior, O. Chalyy, "Study of the ablation stage structure of 1-MA wire arrays with x-ray and UV diagnostics". *The Dense Z-pinches Conference*, Napa, August 4-7, 2014. Oral.
10. A. A. Anderson, V. V. Ivanov, "Investigation of the 3D structure of the Z pinch using UV laser probing", *Annual Meeting of the Far West Section of the APS*, October 23-25, 2014, Reno, Nevada. Poster**.**
11. V. V. Ivanov, D. Papp, A. A. Anderson, B. R. Talbot, A. L. Astanovitskiy, V. Nalajala, O. Dmitriev, J. P. Chittenden, N. Niasse, "Study of bright spots in wire-array z-pinches", *55rd Annual Meeting of the APS Division of Plasma Physics,* Denver, Colorado, Nov.11-15, 2013. Oral.
12. A. Anderson, V. V. Ivanov, D. Papp, B. Talbot, A. Astanovitskiy, "Study of Ablation and Implosion Stages of 1-MA Wire Array Z-Pinch using X-ray Laser-Based Backlighting", *55rd Annual Meeting of the APS Division of Plasma Physics,* Denver, Colorado, November 11-15, 2013. Poster**.**
13. B. R. Talbot, V. V. Ivanov, I. A. Begishev, A. L. Astanovitskiy, V. Nalajala, O. Dmitriev, "Development of the diagnostic laser for deep UV probing of the dense Z-pinch", *55rd Annual Meeting of the APS-DPP,* Denver, Colorado, November 11-15, 2013. Poster**.**
14. A. Anderson, V. Ivanov, B. Talbot, D. Papp", Study of Ablation and Implosion Stages of 1MA Wire Array Z-Pinches Using UV Laser Diagnostics", *IEEE Pulsed Power Plasma Science Conf.,* San Francisco, CA, June 16-21, 2013. Oral.

15. V. V. Ivanov, D. Papp, A. A. Anderson, A. L. Astanovitskiy, O. Dmitriev, V. Nalajala, B. R. Talbot, "Study of dynamics of hot spots in wire-array z-pinches", *IEEE Pulsed Power Plasma Science Conf.,* San Francisco, CA, June 16-21, 2013. Poster**.**
16. D. Papp, V. V. Ivanov, R. Presura, A. A. Anderson, B. R. Talbot, "Specially resolved spectroscopy of HED plasmas using a single convex crystal", *IEEE Pulsed Power Plasma Science Conf.,* San Francisco, CA, June 16-21, 2013. Poster**.**
17. A. A. Anderson, V. V. Ivanov, D. Papp, S. D. Altemara, "Study of Implosion in Wire Arrays with UV interferometry and Faraday Rotation Diagnostics", *Radiation from High Energy Density Plasmas, International Workshop*, Tahoe City, NV April 2013. Poster.
18. D. Papp, V. V. Ivanov, R. Presura, A. A. Anderson, B. R. Talbot, **"**Developing Imaging Spectroscopy of HED Plasmas Using a Single Convex Crystal", *Radiation from High Energy Density Plasmas, International Workshop*, Tahoe City, April 2013. Poster**.**
19. V.V. Ivanov, J.P. Chittenden, R.C. Mancini, D. Papp, N. Niasse, A.A. Andersen, S.D. Altemara, "Study of instabilities in wire-array Z pinches at stagnation", *54th Annual Meeting of the Division of Plasma Physics,* Providence, Rhode Island, October 29-November 2, 2012. Oral.
20. S. D. Altemara, A. A. Anderson, D. Papp, V. Ivanov, "Development of UV Two-Frame Imaging Diagnostics for Investigation of Plasma Dynamics in Z Pinches at Stagnation", *54th Annual Meeting of the Division of Plasma Physics,* Providence, Rhode Island, October 29-November 2, 2012. Oral.
21. D. Papp, V. V. Ivanov, P. Hakel, R. C. Mancini, S. D. Altemara, A. A. Anderson, "Investigation of K-shell radiation from two-component wire arrays", 54th Annual Meeting of the Division of Plasma Physics, Providence, Rhode Island, October 29-November 2, 2012.
22. A. A. Anderson, V. V. Ivanov, D. Papp, S. D. Altemara, "Study of Implosion in Wire Arrays with UV interferometry and Faraday Rotation Diagnostics", *54th Annual Meeting of the Division of Plasma Physics,* Providence, Rhode Island, October 29-November 2, 2012.

### 2.2. Technologies or techniques

Deep UV laser diagnostics for dense plasmas were developed.
Four-color diagnostics was developed to study plasma in a wide range of densities in one shot.
Non-linear picosecond Kerr shutter was tested in application to laser diagnostics of plasma.
Two-plasmon decay was suggested for measurement of strong magnetic fields.
The magnetic field of 2-3 MG generated by the Zebra pulsed power machine was applied to the controlled study of magnetized plasma.

## 3. PARTICIPANTS AND COLLABORATING ORGANIZATIONS

A PI of the project, Dr. V. V. Ivanov coordinated all works and carried experiments. Two PhD graduate students, A.A. Anderson, and D. Papp carried out experiments for the grant program. Students developed x-ray and UV diagnostics, supported other plasma diagnostics, and processed data. We cooperated with the NTF stuff, A. Astanovitskiy, and V. Nalajala. We collaborated with Drs. J. P. Chittenden and N. Niasse from the Imperial College, London for 3D MHD simulations of experiments at NTF. We collaborated with Drs. R.C. Mancini and B.B. Bauer (UNR) in atomic physics and the development of loads for magnetized plasma experiments. We collaborated with Drs. R. Betti, A. Maximov, and I. Begishev from the University of Rochester for the theoretical investigation of laser produced plasma in the MG field and generation of the $5^{th}$ laser harmonic. We collaborated with M. E. Sherrill and P. Hakel (LANL) in x-ray spectroscopy.

## 4. IMPACT

UV and deep UV diagnostics were applied to Z-pinch plasmas. New diagnostics allowed study of the dense plasma which was investigated in previous papers only by x-ray methods. Four-color laser diagnostics were used to study plasma in a wide density range in one laser shot.

New UV diagnostics provided a breakthrough for investigation of the 1-MA Z pinch. MHD instabilities, areas of disruption, and small-scale density perturbations were observed at stagnation in unprecedented details.

High asymmetry of wire-array Z pinches due to the asymmetrical implosion and instabilities was found with a 4-channel shadowgraphy. This is important for interpretation on data from optical and x-ray diagnostics.

MG magnetic fields were measured by the UV Faraday diagnostic in the stagnated Z pinch with current up to 1.5 MA and a profile of current was reconstructed. It was found that a significant part of current can flow in trailing plasma. Secondary implosions of non-imploded plasma generate enhanced kinetic energy and radiation at stagnation. Study of plasma dynamics in the Z pinch showed that stagnation is a dynamic process with fast plasma motion. Secondary implosions, plasma motion, and radiation of hot spots can explain a long lasting mystery of the enhanced energy radiated by the Z pinch.

The origin of bright x-ray spots in Z pinches was studied using UV diagnostics coupled with a streak camera. A collapse of the micropinch on the neck produces a hot spot. A single hot spot generates 1-2% of the Z-pinch energy. All hot spots can radiate 10-20% of the total pinch energy.

A two-plasmon decay of the laser pulse in the magnetized plasma was studied. 3/2ω scattered radiation carry a signature of the magnetic field and may be used for measuring of strong magnetic fields in HED plasmas. Laser plasma interaction in the 2-3 MG external magnetic field was investigated at the first time. Proposal “Laser plasma interaction in the MG magnetic field” was submitted for the DOE-NSF partnership in Basic physics and selected for funding in 2016-2019.

Two PhD students were trained for the HED physics. The researches carried out for this grant impact a Z pinch and basic plasma physics.

## 5. CHANGE/PROBLEM

A non-cost extension was requested due to the problem with a SL221 laser made by Altos Photonics Inc. The re-designed laser was delivered and installed in November, 2015. Finally, all milestones of the grant were passed and research goals accomplished.